International Journal of Fracture **61**: 17–37, 1993.

Green's function for the elastic field of an edge dislocation in a finite orthotropic medium*

A. EL-AZAB and N.M. GHONIEM
Mechanical, Aerospace and Nuclear Engineering Department, 46-147G Eng.IV, University of California, Los Angeles, Los Angeles, California 90024, USA

Received 1 August 1992; accepted in revised form 12 January 1993

Abstract. A fundamental solution of plane elasticity in a finite domain is developed in this paper. A closed-form Green's function for the elastic field of an edge dislocation of arbitrary Burger's vector at an arbitrary point in an orthotropic finite elastic domain, that is free of traction, is presented. The method is based on the classical theory of potential fields, with an additional distribution of surface dislocations to satisfy the free traction boundary condition. A solution is first developed for a dislocation in a semi-infinite half-plane. The resulting field is composed of two parts: a singular contribution from the original dislocation, and a regular component associated with the surface distribution. The Schwarz-Christoffel transformation is then utilized to map the field quantities to a finite, polygonal domain. A closed form solution containing Jacobi elliptic functions is developed for rectangular domains, and applications of the method to problems of fracture and plasticity are emphasized.

1. Introduction

The concept of a dislocation was first introduced by Weingarten [1], Timpe [2] and Volterra [3] as a mathematical device to deal with the possibility of solutions which satisfy the governing equations of the theory of elasticity, but possess the property of a multi-valued displacement field. For many years after its introduction, the mathematical device was termed a Volterra dislocation [4]. On the other hand, the existence of crystal dislocations was found to be necessary for explaining the fact that most ductile materials yield and fail at stress levels that are at least three orders of magnitude smaller than the theoretical values predicted by atomic potential considerations alone [5–8]. The advent of analytical techniques in materials science proved, beyond doubt, the important role which crystal dislocations play in deformation, micromechanics of fracture, and other materials properties. The *materials science* applications of the theory of dislocations are extensively reviewed by Hirth and Lothe [9] and Nabarro [10]. A detailed work on the use of dislocation theory in modelling materials phenomena such as twining, grain boundaries [11, 12], interfacial energy and surface tension [13, 14] was conducted by Marcinkowski and Jagannadham. More recently, Amodeo and Ghoniem [15, 16] developed a dynamical method for the study of the micromechanics of plasticity in ductile materials. They termed their method *Dislocation Dynamics*, in which they solved for the simultaneous equations of motion of distributions of dislocations under a variety of applied stress conditions. In their work, however, they used elasticity solutions for dislocations in an infinite isotropic medium.

Applications of dislocation theory to fracture mechanics, deals with dislocations in a continuum. The continuum theory of dislocations is reviewed by Hirth and Lothe [9], Nabarro

*This material is based upon work supported by the Department of Energy under Award number DE-FG03-91ER54115 at UCLA.

[10], Mura [17, 18], and Lardner [19]. In fracture applications closed form solutions can be obtained by modeling cracks by continuous (or discrete) distributions of dislocations. However, the proper dislocation elastic fields (Green's function) in the crack domain must be available. Examples on application of dislocation theory to fracture mechanics are reported by A.N. Stroh [20], J. Qu and Q. Li [21], J.R. Willis [22], Delale and Erdogan [23], Lardner [24], Atkinson [25], and Vitek [26]. A review of dislocation models in fracture is given by Lardner [19], Vitek and Chell [27], Jagannadham and Marcinkowski [28] and Bilby and Eshelby [29], where dislocation Green's functions developed for infinite domains were used. In [28] extensive use of dislocation theory in modeling elastic and elastic–plastic fracture problems has been made.

In some cases dislocation fields are obtained for finite (circular, infinite strip of finite width) domains using the image dislocation method [9, 10]. Marcinkowski et al. [30] argued that the image dislocation method is inadequate to obtain dislocational fields in finite domains since the resulting elastic fields do not vanish outside the domain of solution. They also introduced the method of surface dislocations to obtain dislocation fields in semi-infinite domains. The idea of the surface dislocation technique is based on the use of a correcting field, which yields the field in a finite domain if added to the infinite domain solution, with the boundary conditions satisfied. Marcinkowski et al. [30, 31] used distributions of dislocations along a semi-infinite domain boundary to generate the additional correcting field. They developed analytical expressions for edge dislocations in *isotropic* half-planes. Their method proved to be exact and realistic in the sense that the dislocation fields identically vanish outside and on the domain boundaries. For rectangular domains, they used numerical methods to obtain the solution [32]. These approaches are based upon the classical theory of potential fields, and rely on solving an integral equation for the surface dislocation distribution. Other authors obtained the dislocation fields in half-space using the analytic continuation technique [33, 34]. In this method, additional correcting fields are determined so as to satisfy the free traction boundary condition on the domain boundary. However, Miller [33] and J.C. Lee [34] used two different methods to find the correcting fields, which yielded different expressions.

In applying dislocation theory to fracture mechanics or other materials science phenomena, the importance of development of an accurate solution to the governing equations of elasticity for a dislocation cannot be underestimated. It is from this perspective that we develop our present dislocation Green's function in a finite orthotropic domain. The problem formulation makes use of the classical theory of potential fields, with the surface dislocation technique to obtain the solution in a half-plane. The Schwarz-Christoffel transformation [35–37] is then utilized to obtain the solution in a finite (rectangular) domain. As will be shown here, only the elastic field of a dislocation in an infinite domain is a necessary ingredient in our present formulation.

2. Green's function for the elastic field of a dislocation in an infinite domain

For an elastic anisotropic continuum with material constants s_{mn} $(m, n = 1, 2, 6)$ Hooke's law is written as

$$\begin{aligned} \varepsilon_x &= s_{11}\sigma_x + s_{12}\sigma_y + s_{16}\sigma_{xy}, \\ \varepsilon_y &= s_{12}\sigma_x + s_{22}\sigma_y + s_{26}\sigma_{xy}, \\ 2\varepsilon_{xy} &= s_{16}\sigma_x + s_{26}\sigma_y + s_{66}\sigma_{xy}. \end{aligned} \tag{1}$$

The stresses and complex displacement $\mathscr{U}$ are written in terms of the complex potentials, $\phi_1(z_1)$ and $\phi_2(z_2)$ as follows [33, 34]

$$\begin{aligned}
\sigma_x &= 2\,\mathrm{Re}[\lambda_1^2\phi_1'(z_1) + \lambda_2^2\phi_2'(z_2)],\\
\sigma_y &= 2\,\mathrm{Re}[\phi_1'(z_1) + \phi_2'(z_2)],\\
\sigma_{xy} &= -2\,\mathrm{Re}[\lambda_1\phi_1'(z_1) + \lambda_2\phi_2'(z_2)],\\
\mathscr{U} &= p(\lambda_1)\phi_1(z_1) + p(\lambda_2)\phi_2(z_2) + p(\bar{\lambda}_1)\bar{\phi}_1(\bar{z}_1) + p(\bar{\lambda}_2)\bar{\phi}_2(\bar{z}_2),
\end{aligned} \tag{2}$$

in which Re = *real of* and the overbar represents complex conjugation. The primed variables are derivatives with respect to z_1 or z_2. The constants λ_1 and λ_2 and their complex conjugates are the roots of the following characteristic equation [38]

$$s_{11}\lambda^4 - 2s_{16}\lambda^3 + (2s_{12} + s_{66})\lambda^2 - 2s_{26}\lambda + s_{22} = 0 \tag{3}$$

and z_1 and z_2 are complex variables defined as

$$\begin{aligned}
z_1 &= x + \lambda_1 y = (\gamma_1 z + \delta_1 \bar{z})/2,\\
z_2 &= x + \lambda_2 y = (\gamma_2 z + \delta_2 \bar{z})/2,
\end{aligned} \tag{4}$$

where $z = x + iy$, $\gamma_j = 1 - i\lambda_j$ and $\delta_j = 1 + i\lambda_j, j = 1, 2$. The functions $\phi_1(z_1)$ and $\phi_2(z_2)$ are the complex potentials of the dislocation and are analytic within the body except at z_0. The polynomial $p(\lambda)$ is given by [38]

$$p(\lambda) = (s_{12} - s_{16}\lambda + s_{11}\lambda^2) + \frac{i}{\lambda}(s_{22} - s_{26}\lambda + s_{12}\lambda^2). \tag{5}$$

The complex potentials at a point z (*or alternatively* $z_{1,2}$) due to a single dislocation at $z_0 = x_0 + iy_0$ in an infinite anisotropic plane are given by [33, 34]

$$\begin{aligned}
\phi_{1s}(z_1) &= A_1 \log(z_1 - z_{10}),\\
\phi_{2s}(z_2) &= A_2 \log(z_2 - z_{20}),
\end{aligned} \tag{6}$$

where z_{10} and z_{20} are related to z_0 by the set of equations (4). The subscript s is added to indicate that the infinite domain potentials are *singular* at the location of the dislocation z_0. The complex constants $A_{1,2}$ are determined by the conditions that the deformation due to a single dislocation is *not* single-valued (*dislocational*), and the traction integral along any arbitrary contour surrounding the dislocation vanishes (*self-equilibrium*). The dislocation condition can be expressed as

$$b = 2\pi i[p(\lambda_1)A_1 - p(\bar{\lambda}_1)\bar{A}_1 + p(\lambda_2)A_2 - p(\bar{\lambda}_2)\bar{A}_2], \tag{7}$$

where $b = |b|\,e^{i\theta}$ is the Burger's vector of the dislocation. The self-equilibrium condition yields the following equation

$$\delta_1 A_1 - \bar{\gamma}_1 \bar{A}_1 + \delta_2 A_2 - \bar{\gamma}_2 \bar{A}_2 = 0. \tag{8}$$

Derivations of the last two equations are found in Appendix A. By taking the complex conjugate of (7) and (8), two additional equations are obtained. The four equations can be solved for A_1, $\bar{A}_1$, A_2 and $\bar{A}_2$. Appendix B contains a solution for A_1 and A_2 for the case of an *orthotropic* domain, where $s_{16} = s_{26} = 0$, which is written as

$$\begin{aligned} A_1 &= c_{11}\,\mathrm{Im}(b) + ic_{12}\,\mathrm{Re}(b), \\ A_2 &= c_{21}\,\mathrm{Im}(b) + ic_{22}\,\mathrm{Re}(b), \end{aligned} \tag{9}$$

where c_{ij} are *real* constants which depend on the material constants s_{mn}. Re(b) and Im(b) are the real and imaginary parts of the Burger's vector, respectively.

3. Dislocation in a finite domain: General formulation

Consider an edge dislocation of arbitrary Burger's vector, $b = |b|\,e^{i\theta}$, which is located at z_0 in the finite domain D^+ bounded by the coutour L, as shown in Fig. 1. *The Green's function in an unbounded medium automatically satisfies the governing field equations. Any linear combination of the infinite domain Green's functions, which also satisfies specified boundary conditions for a finite domain, must be the Green's function in that finite domain.* The solution, therefore, will be constructed as a linear combination of the singular, infinite domain solution, and an additional distribution of surface dislocations, such that the boundary is free of forces (i.e. zero surface tractions).

Let $F(t)$ be a distribution function of surface dislocations, which is complex, and written as

$$F(t) = f_1(t) + if_2(t), \tag{10}$$

where t is a complex variable describing the domain boundary L, and $f_1(t)$ and $f_2(t)$ are real functions of the complex variable t. Physically, $F(t)\,ds$ is defined as the Burger's vector of the surface dislocation in the interval ds, where $s = s(t)$ is the scalar distance along the domain boundary. The traction caused by the original dislocation and the surface distribution, evaluated at any arbitrary point along the boundary, must be equal to any prescribed boundary tractions. For the case of a free surface, this condition is written as

$$X_d(t) + iY_d(t) + \oint_L [X_s(t_0, t) + iY_s(t_0, t)]\,ds_0 = 0, \tag{11}$$

where $s_0 = s(t_0)$ and $X_d + iY_d$ is the residual complex traction at t on L due to the original dislocation at z_0 inside D^+. $X_s(t_0, t) + iY_s(t_0, t)$ is the complex traction at t on L due to a surface dislocation of Burger's vector $F(t_0)$ at t_0 on L. If the surface experiences any localized or distributed forces, $T(t)$, the right hand side of (11) is no longer zero, but rather $= T(t)$. Here, we consider only free surfaces. Equations (2), (6) and (9) will be used to determine $X_d + iY_d$ at any point t on L. The same equations will be used to determine $X_s(t_0, t) + iY_s(t_0, t)$ at t on L, with one difference, that is; Re(b) and Im(b) in (9) will be replaced

by $f_1(t_0)$ and $f_2(t_0)$. This means that the complex quantities A_1 and A_2 are no longer constants when dealing with surface dislocations. Let these quantities be denoted by B_1 and B_2, and be written as

$$B_1(t) = c_{11}f_2(t) + ic_{12}f_1(t),$$
$$B_2(t) = c_{21}f_2(t) + ic_{22}f_1(t). \tag{12}$$

Equation (11) can now be rewritten in terms of $f_1(t)$ and $f_2(t)$, and can be utilized to determined these two functions. Once $f_1(t) + if_2(t)$ is determined, the total stress field can be determined at any point in the domain D^+ by adding together the singular field and the additional field due to surface dislocations.

When a rectangular domain is considered, as shown in Fig. 2, two mathematical difficulties arise;

(1) the residual singular traction, $X_d + iY_d$, will have different expressions as t describes different sides of the rectangle, and
(2) the contour L is not smooth.

Because of that, a suitable numerical method may be used to solve (11) and (12) for the complex function $f_1(t) + if_2(t)$. Such an approach was used by Jagannadham and Marcinkowski [32], to predict the stress field for an edge dislocation in an *isotropic* rectangular domain. Their solution yielded inaccurate results outside and close to the domain boundary, and they were able to satisfy the boundary coonditions in an approximate point collocation fashion. The reader is advised to compare the present results with those of [32]. From the mathematical point of view, there is an inherent difficulty associated with the problem of finding the elastic field of a dislocation in a polygonal domain. As can be noticed from the forms of the functions $\phi_1(z_1)$ and $\phi_2(z_2)$, the field is a cylindrical potential field, which is to be fit onto a geometrically incompatible polygonal boundary. However, the approach taken here is to obtain the solution in a semi-infinite domain and then use the Schwarz-Christoffel transformation to map the solution onto a polygon. This approach is illustrated in the next two sections.

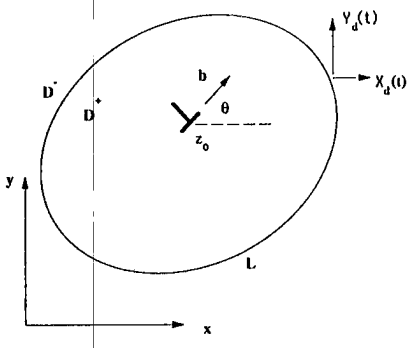

Fig. 1. Arbitrary dislocation in a finite domain.

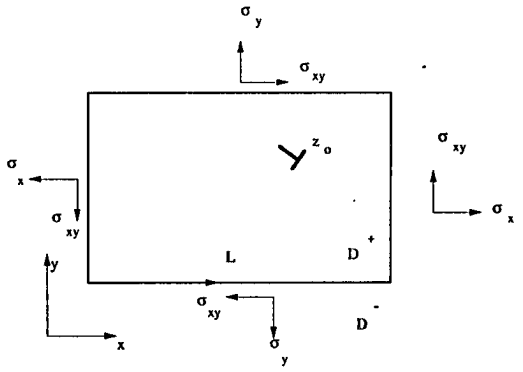

Fig. 2. Variation of the residual surface traction for a dislocation in a rectangular domain.

4. Dislocation solution in an orthotropic semi-infinite domain

4.1. Distribution function of surface dislocations

Consider a dislocation of an arbitrary Burger's vector $b = |b| e^{j\theta}$ at the point $z_0 = x_0 + iy_0$, as shown in Fig. 3. The domain of solution D^+ is the upper half-plane, $\mathrm{Im}(z) \geqslant 0$, so that the contour L is taken to be the x-axis from $-\infty$ to $+\infty$. In this case the residual singular traction $X_d(t) + iY_d(t)$ is given by

$$X_d(t) + iY_d(t) = \sigma_{xy}(z_0, x) + i\sigma_y(z_0, x), \tag{13}$$

similarly,

$$X_s(t_0, t) + iY_s(t_0, t) = \sigma_{xy}(x_0, x) + i\sigma_y(x_0, x), \tag{14}$$

so that (11) is rewritten as

$$\sigma_{xy}(z_0, x) + i\sigma_y(z_0, x) + \int_{-\infty}^{+\infty} (\sigma_{xy}(x_0, x) + i\sigma_y(x_0, x))\, \mathrm{d}x_0 = 0. \tag{15}$$

Using (2), for stresses in terms of the complex potentials, expressions for $\sigma_{xy}(z_0, x)$ and $\sigma_y(z_0, x)$ are written as

$$\begin{aligned} \sigma_{xy}(z_0, x) &= -2\,\mathrm{Re}\left[\frac{\lambda_1 A_1}{x - z_{10}} + \frac{\lambda_2 A_2}{x - z_{20}}\right], \\ \sigma_y(z_0, x) &= 2\,\mathrm{Re}\left[\frac{A_1}{x - z_{10}} + \frac{A_2}{x - z_{20}}\right], \end{aligned} \tag{16}$$

where $A_{1,2}$ are given by (9). Similar expressions can be written for $\sigma_{xy}(x_0, x)$ and $\sigma_y(x_0, x)$, by replacing A_1 and A_2 and B_1 and B_2 given by (12). The result is stated as follows

$$\begin{aligned} \sigma_{xy}(x_0, x) &= -2\,\mathrm{Re}\left[\frac{\lambda_1 B_1(x_0)}{x - x_0} + \frac{\lambda_2 B_2(x_0)}{x - x_0}\right], \\ \sigma_y(x_0, x) &= 2\,\mathrm{Re}\left[\frac{B_1(x_0)}{x - x_0} + \frac{B_2(x_0)}{x - x_0}\right]. \end{aligned} \tag{17}$$

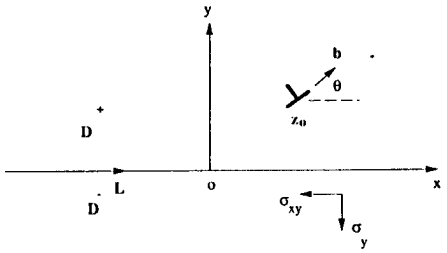

Fig. 3. Dislocation in a semi-infinite domain.

If (12) is used in (17), the following simplified expressions for $\sigma_{xy}(x_0, x)$ and $\sigma_y(x_0, x)$ are obtained for the case of *orthotropic* domains

$$\sigma_{xy}(x_0, x) = \frac{2(\beta_1 c_{12} + \beta_2 c_{22}) f_1(x_0)}{x - x_0} = \frac{a_1 f_1(x_0)}{x - x_0},$$
$$\sigma_y(x_0, x) = \frac{2(c_{11} + c_{21}) f_1(x_0)}{x - x_0} = \frac{a_2 f_2(x_0)}{x - x_0}, \tag{18}$$

where σ_{xy} and σ_y in (16) and (18) are real quantities. β_1 and β_2 are the imaginary parts of the roots λ_1 and λ_2. Note that λ_1 and λ_2 are pure imaginary in the case of orthotropic materials (see Appendix B).

The integral equation (15) can then be rewritten as

$$\sigma_{xy}(z_0, x) + i\sigma_y(z_0, x) + \int_{-\infty}^{+\infty} \frac{a_1 f_1(x_0) + i a_2 f_2(x_0)}{x - x_0} \mathrm{d}x_0 = 0, \tag{19}$$

which is a singular integral equation with a Cauchy-type kernel. The integral part exists in the sense of its principal value. The integral equation (19) can be directly solved for $a_1 f_1(x) + i a_2 f_2(x)$. Alternatively, the real and imaginary parts of the integral equation can be separated to obtain two real integral equations for $f_1(x)$ and $f_2(x)$. Following Muskhelishvili's methods for the solution of singular integral equations [39, 40], and excluding mathematical details, the following two expressions are obtained for $f_1(x)$ and $f_2(x)$

$$f_1(x) = \frac{-i}{\pi a_1}\left[\frac{\lambda_1 A_1}{x - z_{10}} - \frac{\bar{\lambda}_1 \bar{A}_1}{x - \bar{z}_{10}} + \frac{\lambda_2 A_2}{x - z_{20}} - \frac{\bar{\lambda}_2 \bar{A}_2}{x - \bar{z}_{20}}\right],$$
$$f_2(x) = \frac{i}{\pi a_2}\left[\frac{A_1}{x - z_{10}} - \frac{\bar{A}_1}{x - \bar{z}_{10}} + \frac{A_2}{x - z_{20}} - \frac{\bar{A}_2}{x - \bar{z}_{20}}\right], \tag{20}$$

where $f_1(x)$ and $f_2(x)$ are real quantities. The complex function $F(x) = f_1(x) + i f_2(x)$ must satisfy overall material compatibility condition, i.e. conservation of Burger's vector [30], which can be examined using the following integral

$$\int_{-\infty}^{x} F(x')\,\mathrm{d}x' = b_s(x)$$

$$b_s(x) = -b + \left(\frac{-i}{\pi a_1}\right)[\lambda_1 A_1 \log(x - z_{10}) - \bar{\lambda}_1 \bar{A}_1 \log(x - \bar{z}_{10})$$
$$+ \lambda_2 A_2 \log(x - z_{20}) - \bar{\lambda}_2 \bar{A}_2 \log(x - \bar{z}_{20})],$$
$$+ \left(\frac{-1}{\pi a_2}\right)[A_1 \log(x - z_{10}) - \bar{A}_1 \log(x - \bar{z}_{10})$$
$$+ A_2 \log(x - z_{20}) - \bar{A}_2 \log(x - \bar{z}_{20})]. \tag{21}$$

It can be shown that $b_s(x) \to -b$ as $x \to +\infty$.

The results are specialized for an orthotropic domain for which $s_{16} = s_{26} = 0$. To test the theory presented here, the properties of the Nicalon/CVD-SiC (fiber/matrix), which is an orthotropic material, are chosen. The elastic constants are evaluated using the rule of mixture for the fiber and matrix properties given in [42, 43]. The plane stress compliance constants are determined to be $s_{11} = 3.125 \times 10^{-12}$, $s_{22} = 3.503 \times 10^{-12}$, $s_{12} = -6.563 \times 10^{-13}$, and $s_{66} = 9.31 \times 10^{-12}\,\text{Pa}^{-1}$.

In presenting the results all distances are normalized to the magnitude of the Burger's vector. Figure 4 shows a typical surface distribution as a function of the distance along the free surface, for a dislocation at $z_0 = +i50$ with a purely real Burger's vector. It is obvious that $F(x) \to 0$ as $x \to \pm\infty$. The effect of varying the distance y_0 from the free surface on $|F(x)|$ is shown in Fig. 5. The distribution becomes sharper as y_0 becomes smaller and localized at $x = 0$. It also broadens as y_0 becomes large. In fact, this is a fundamental difference between the surface dislocation technique and the image dislocation method for which the image dislocation represents an extremely localized distribution at the point $x = 0$. In Fig. 6, the integral surface Burger's vector $b_s(x)$, which is given by (21) is shown on an Argand diagram for different orientation of the Burger's vector of the lattice dislocation. x describes one curve as it varies from $-\infty$ to $+\infty$. $b_s(x)$ is given by the vector drawn from the point (0, 0) to any point on a curve. The results

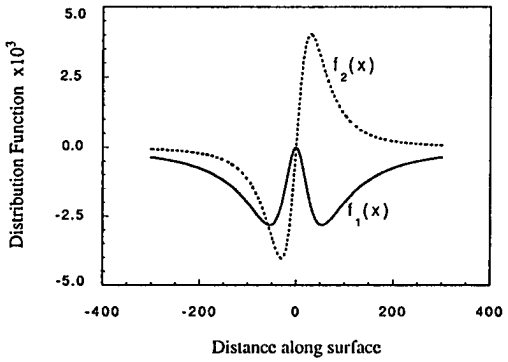

Fig. 4. The surface distribution ($F(x) = f_1(x) + if_2(x)$) as a function of distance along the surface. $z_0 = +i50$. The Burger's vector is real.

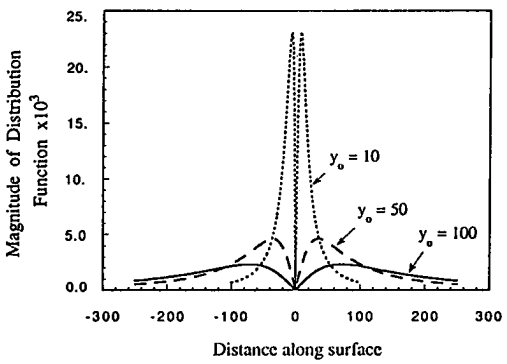

Fig. 5. Magnitude of $F(x)$ as a function of distance along the surface for different positions of the dislocation ($z_0 = +iy_0$). The Burger's vector is real.

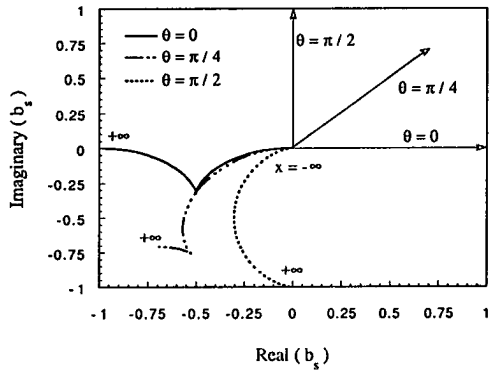

Fig. 6. Argand diagram for b_s as given by (21) for three different orientations of the Burger's vector b. The curves represent $b_s(x)$, where x varies form $-\infty$ to $+\infty$. The arrows represent the Burger's vectors b of the lattice dislocation. As $x \to +\infty b_s \to -b$.

clearly indicate that the condition of material compatibility is satisfied. That is to say $b + \int_{-\infty}^{+\infty} F(x')\,dx' = 0$ [30].

4.2. Field quantities in a semi-infinite domain

The complex potentials due to surface dislocations will be denoted by $\phi_{1r}(z_1)$ and $\phi_{2r}(z_2)$. These potentials will be evaluated as integrals over the distribution function of surface dislocation on x-axis, as follows

$$\phi_{jr}(z_j) = \int_{-\infty}^{+\infty} B_j(x) \log(z_j - x)\,dx, \tag{22}$$

where $j = 1, 2$. Since the stresses are determined in terms of the derivatives of two complex potentials, it is convenient to develop an expression for $\phi'_{jr}(z_j)$, which is written as

$$\phi'_{jr}(z_j) = \int_{-\infty}^{+\infty} \frac{B_j(x)}{z_j - x}\,dx, \tag{23}$$

where, again, B_j is determined in terms of $f_1(x)$ and $f_2(x)$ using (12). Omitting mathematical details, expressions for $\phi'_{1r}(z_1)$ and $\phi'_{2r}(z_2)$ are obtained as follows

$$\begin{aligned}
\phi'_{1r}(z_1) &= \left(\frac{2ic_{12}}{a_1}\right)\left[\frac{\bar{\lambda}_1\bar{A}_1}{z_1 - \bar{z}_{10}} + \frac{\bar{\lambda}_2\bar{A}_2}{z_1 - \bar{z}_{20}}\right] + \left(\frac{-2c_{11}}{a_2}\right)\left[\frac{\bar{A}_1}{z_1 - \bar{z}_{10}} + \frac{\bar{A}_2}{z_1 - \bar{z}_{20}}\right]; \quad (z_1 \in D^+), \\
&= \left(\frac{2ic_{12}}{a_1}\right)\left[\frac{\lambda_1 A_1}{z_1 - z_{10}} + \frac{\lambda_2 A_2}{z_1 - z_{20}}\right] + \left(\frac{-2c_{11}}{a_2}\right)\left[\frac{A_1}{z_1 - z_{10}} + \frac{A_2}{z_1 - z_{20}}\right]; \quad (z_1 \in D^-),
\end{aligned} \tag{24}$$

$$\begin{aligned}
\phi'_{2r}(z_2) &= \left(\frac{2ic_{22}}{a_1}\right)\left[\frac{\bar{\lambda}_1\bar{A}_1}{z_2 - \bar{z}_{10}} + \frac{\bar{\lambda}_2\bar{A}_2}{z_2 - \bar{z}_{20}}\right] + \left(\frac{-2c_{21}}{a_2}\right)\left[\frac{\bar{A}_1}{z_2 - \bar{z}_{10}} + \frac{\bar{A}_2}{z_2 - \bar{z}_{20}}\right]; \quad (z_2 \in D^+), \\
&= \left(\frac{2ic_{22}}{a_1}\right)\left[\frac{\lambda_1 A_1}{z_2 - z_{10}} + \frac{\lambda_2 A_2}{z_1 - z_{20}}\right] + \left(\frac{-2c_{21}}{a_2}\right)\left[\frac{A_1}{z_2 - z_{10}} + \frac{A_2}{z_2 - z_{20}}\right]; \quad (z_2 \in D^-).
\end{aligned} \tag{25}$$

The two derivatives $\phi'_{jr}(z_j), j = 1, 2$ are *regular* everywhere in the entire z_1 and z_2 (or z) planes, including boundary points because the poles lie outside the respective domains. The total field is now constructed as the superposition of *the singular and regular fields*, as follows

$$\phi'_j(z_j) = \phi'_{js}(z_j) + \phi'_{jr}(z_j), \tag{26}$$

where $\phi'_{js}(z_j)$ are given by (6). The stress tensor components in the half-plane are given by (2), where derivatives of the complex potential functions are given by (26). With some laborious algebra, the derivatives of the total potentials given by (26) can be shown to be identically zero at any point in the lower half-plane ($\mathrm{Im}(z) \leqslant 0$). The stress tensor components, σ_x, σ_y and σ_{xy}, will therefore vanish outside the domain boundary.

Figures 7, 8 and 9 show equi-stress contours for different stress components for a dislocation in a semi-infinite domain. x and y refer to the real and imaginary axes of the complex z-plane, respectively. The stresses and distances are normalized to the shear modulus $G_{12} = 1/s_{66}$, of the material, and the magnitude of the Burger's vector, respectively. Only zero stress contours of the stress components σ_y and σ_{xy} intersect with the boundary (real-axis), which means that the stress field satisfies the free traction boundary condition. These results illustrate the usefulness of the powerful complex potential field theory, when contrasted with the method of image dislocations [9], analytic continuation techniques [33, 34] and spectral expansion methods [41]. In the immediate neighborhood of the dislocation, the singular stress component (infinite domain field) dominates, which is clearly shown by the behavior of the contour lines close to the point z_0.

5. Green's function for the elastic field of a dislocation in a rectangular orthotropic domain

In this section the Schwarz-Christoffel transformation, which maps the upper half-plane onto a polygon, will be applied to the semi-infinite domain solution to obtain the solution in a rectangular domain. We will consider the case where the boundaries of the rectangular domain

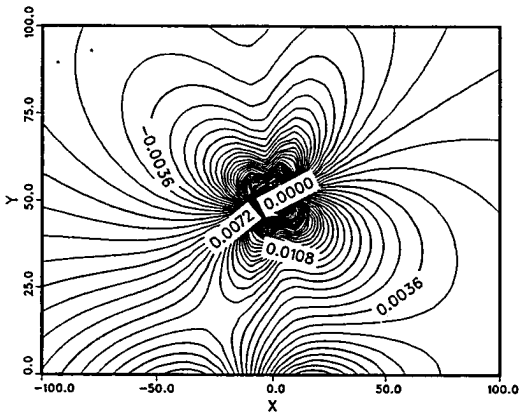

Fig. 7. σ_x for a dislocation ($b = e^{i\pi/4}, z_0 = +50i$) in a semi-infinite domain. The free surface is the real axis.

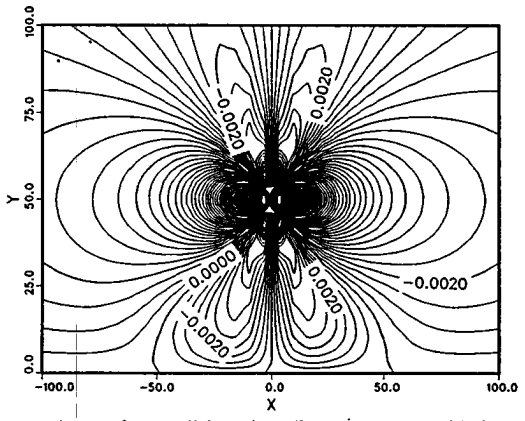

Fig. 8. σ_{xy} for a dislocation ($b = e^{i\pi}, z_0 = +50i$) in a semi-infinite domain. Only zero stress contours intersect with the free surface (real axis).

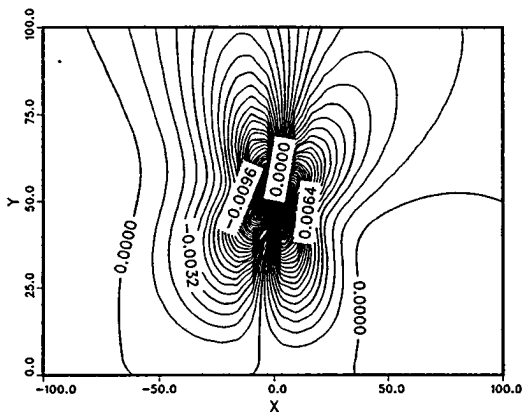

Fig. 9. σ_y for a dislocation ($b = e^{i\pi/4}, z_0 = +50i$) in a semi-infinite domain. Only zero stress contours intersect with the free surface (real axis).

are free of tractions. If a set of surface tractions are subsequently applied, a convenient method can be used, and the total solution is obtained by superposition.

5.1. The Schwarz-Christoffel transformation

The general form of the Schwarz-Christoffel transformation is written as [35–37]

$$w = f(z) = C_1 \int_0^z \prod_{j=1}^{n} (z - a_j)^{\alpha_j - 1}\, dz + C_2. \tag{27}$$

This transformation maps the upper half of the z-plane onto a polygon on n vertices in the w-plane. $C_{1,2}$ are complex constants which adjust the size, orientation and location of the polygon. The points a_j on the x - axis (z-plane) transform to the vertices of the polygon, and $\alpha_j \pi$ are the interior angles of the polygon. With this transformation, solutions in polygonal domains (e.g. hexagons, pentagons, etc) can be obtained from the semi-infinite domain solution.

In the special case of a rectangle, $\alpha_j = \frac{1}{2}$, and $n = 4$. Equation (27) can be written as [36]

$$\begin{aligned} w &= f(z) = \int_0^z \frac{d\xi}{\sqrt{(1 - \xi^2)(1 - k^2\xi^2)}} \\ &= F(z, k); \quad 0 < k < 1 \end{aligned} \tag{28}$$

where $F(z, k)$ is the elliptic integral of the first kind [44, 55]. The integral (28) maps the upper half of the z-plane onto a rectangle in the w-plane for any k, Fig. 10. The vertices of the rectangle in the w-plane are $\pm K(k)$ and $+ iK(k')$; $k^2 + k'^2 = 1$, where $K(k)$ is a complete elliptic integral of the first kind, which is written as

$$K(k) = \int_0^1 \frac{d\xi}{\sqrt{(1 - \xi^2)(1 - k^2\xi^2)}} \tag{29}$$

and $K(k')$ is the complementary complete elliptic integral of the first kind defined by (29) for k'. The vertices of the rectangle are mapped to the points ± 1 and $\pm 1/k$, on the x-axis in the z-plane.

Let the actual rectangular domain which contains the dislocation be defined in the w^*-plane, where $w^* = u^* + iv^*$, as shown in Fig. 10. Let the vertices of the rectangle be given by $\pm H_1$ and $\pm H_1 + iH_2$, which correspond to the four vertices in the w-plane. Consequently, it is necessary to establish a relationship between the w^*-plane and the w-plane before actually using (28) to perform the mapping. In fact the mapping process will be multi-step, from w^*-plane to the w-plane, and then to the z-plane. Let the w^* and the w (where $w = u + iv$) be related as follows

$$\begin{aligned} u^* &= \frac{H_1}{K(k)} u, \\ v^* &= \frac{H_2}{K(k')} v, \\ w^* &= u^* + iv^* = \frac{H_1}{K(k)} u + i \frac{H_2}{K(k')} v. \end{aligned} \tag{30}$$

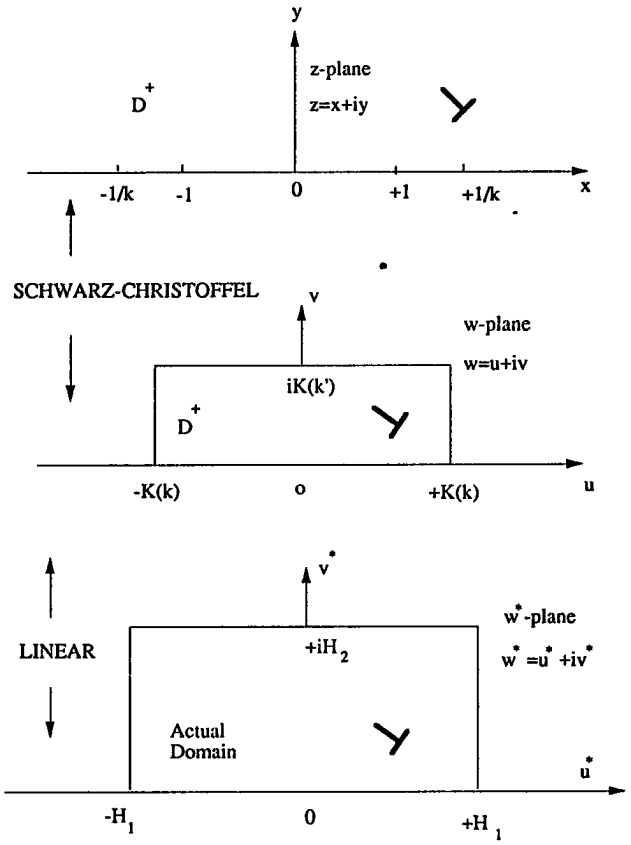

Fig. 10. Schematic of the different complex planes and their interrelationships.

If we arbitrarily choose $H_1/K(k) = H_2/K(k') = c$, i.e. $w^* = cw$, then the transformation between the w^* and w-planes is linear, where the constant c will be determined once the parameter k is determined. The latter is found by solving the following transcendental equation

$$\frac{H_2}{H_1} = \frac{K(k')}{K(k)}, \tag{31}$$

where $k^2 + k'^2 = 1$.

5.2. *Field quantities in a rectangular domain*

The fundamental stress combinations, Θ_z and Φ_z, in the z-plane are written as [38, 39]

$$\Theta_z = \sigma_y + \sigma_x, \tag{32}$$
$$\Phi_z = \sigma_y - \sigma_x + 2i\sigma_{xy}.$$

Under conformal transformation from the z-plane to the w-plane, the fundamental stress combinations transform according to the following relations

$$\Theta_w = \Theta_z, \qquad \Phi_w = \Phi_z e^{2i\psi}. \tag{33}$$

It is clear that Θ_z is an invariant of the transformation, while Φ_z has the transformation Jacobian given by

$$e^{2i\psi} = \left(\frac{dz}{dw}\right) \Big/ \left(\frac{\overline{dz}}{dw}\right). \tag{34}$$

The stress components in the w-plane are determined in terms of Θ_w and Φ_w as follows

$$\sigma_u = \frac{\Theta_w}{2} - \tfrac{1}{4}(\Phi_w + \bar{\Phi}_w),$$

$$\sigma_v = \frac{\Theta_w}{2} + \tfrac{1}{4}(\Phi_w + \bar{\Phi}_w), \tag{35}$$

$$\sigma_{uv} = -\tfrac{1}{4}i(\Phi_w - \bar{\Phi}_w).$$

Since the transformation between the w and w^* plane is linear, the constant c is real, the corresponding Jacobian is unity and, in turn, the field quantities are identical in these two planes. The derivative dz/dw is found from (28) as

$$\frac{dz}{dw} = \sqrt{(1 - z^2)(1 - k^2 z)}. \tag{36}$$

The transformation works as follows: to determine the stress field at a point w^*, w is found using (30) as $w = w^*/c$ then the inverse of the relation (28) is used to find z. Once z is determined, (32) through (35) are used to completely determine the stress field in the w-plane (i.e. in the w^*-plane). The inverse of the relation (28) is known as *the Jacobi elliptic sine function*, which is written as follows

$$z = sn(w, k). \tag{37}$$

The form of the elliptic sine function, and the associated numerical accuracy of the computation are given in Appendix C. Note that the dislocation solution in the w-plane is recovered from the solution in the z-plane. Let the displacement vector in the z- and w-planes be denoted by $\mathcal{U}_z$ and $\mathcal{U}_w$, respectively. The displacement vector transforms as

$$\mathcal{U}_z = \mathcal{U}_u e^{i\psi}. \tag{38}$$

The Burger's vectors must have the same relation. Let the Burger's vector in the z- and w-planes be denoted by b_z (at the point z_0) and b_w (at the point w_0), respectively. Therefore, the Burger's vector in the z-plane is given by.

$$b_z = b_w \, e^{i\psi}, \tag{39}$$

where b_w is the prescribed one, and ψ is given by (34) evaluated at z_0.

6. Discussion and conclusions

Representative results for the stress field in a rectangular orthotropic domain are shown in Figs. 11 through 16. u^* and v^* refer to the real and imaginary axes of the complex w^*-plane, which is the actual domain of the dislocation. The stresses are normalized to the shear modulus G_{12}. In calculating the stress field a value of $k^2 = 0.5$ is chosen, for which $K(k) = K(k') = 1.85407467$. It

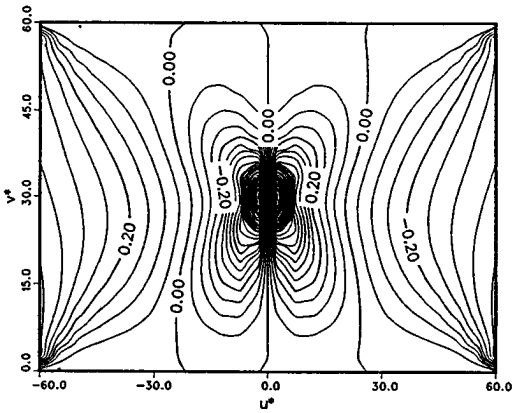

Fig. 11. σ_{v^*} for a dislocation ($b = e^{i\pi/2}$, $w_0^* = +30i$) in a rectangular domain. σ_{v^*} identically vanishes on the upper and lower sides of the rectangle.

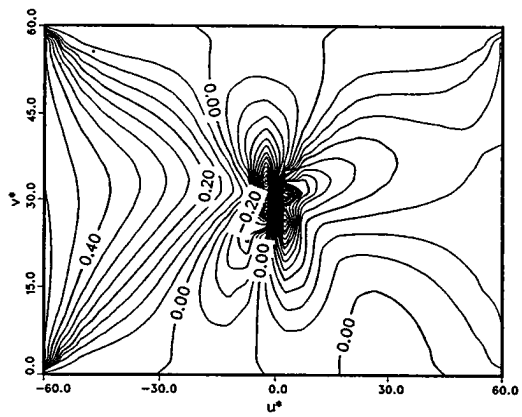

Fig. 12. σ_{v^*} for a dislocation ($b = e^{i\pi/6}$, $w_0^* = +30i$) in a rectangular domain. σ_{v^*} identically vanishes on the upper and lower sides of the rectangle.

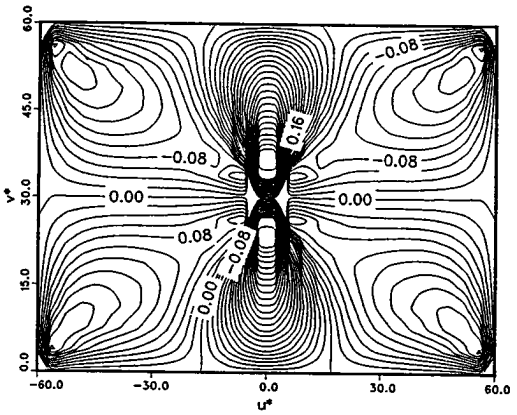

Fig. 13. $\sigma_{u^*v^*}$ for a dislocation ($b = e^{i\pi/2}$, $w_0^* = +30i$) in a rectangular domain. $\sigma_{u^*v^*}$ identically vanishes on all sides of the rectangle.

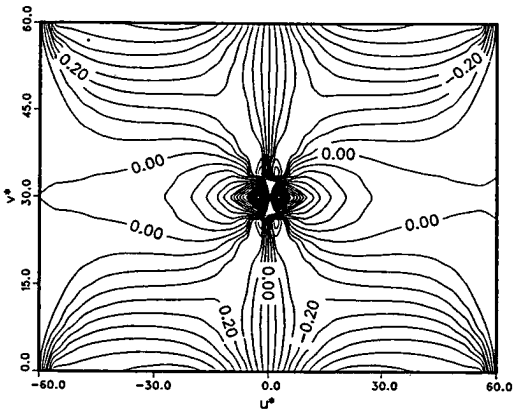

Fig. 14. σ_{u^*} for a dislocation ($b = e^{i\pi/2}$, $w_0^* = +30i$) in a rectangular domain. σ_{u^*} identically vanishes on the right and left sides of the rectangle.

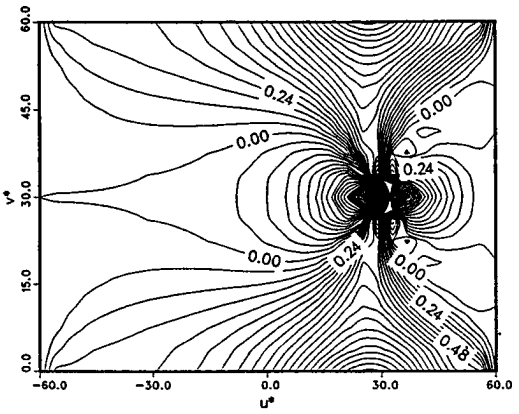

Fig. 15. σ_{u^*} for a dislocation ($b = e^{i\pi/2}$, $w_0^* = 30 + 30i$) in a rectangular domain. σ_{u^*} identically vanishes on the right and left sides of the rectangle.

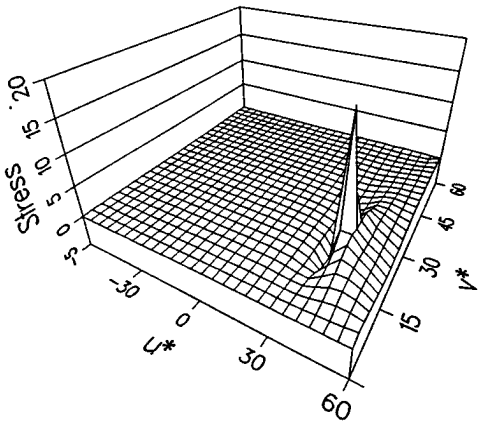

Fig. 16. σ_{v^*} for a dislocation ($b = e^{i\pi/2}$, $w_0^* = 40 + 30i$) in a rectangular domain, showing the singular behavior of the stress field at w_0^*.

is important to note that the shear and normal stresses identically vanish on the domain boundary. Also, the stress field shows the proper singularity at the location of the dislocation (Fig. 16).

The solution presented here is general in the sense that it accounts for the domain orthotropy and geometry effects, which is an essential factor in boundary value problems of elasticity, as well as the arbitrariness in specifing the Burger's vector (magnitude and direction). The solution can be easily extended to domains of general anisotropy. With this solution, a large number of materials macro/micromechanics problems can be accurately treated in the sense that more realistic dislocational fields in domains of finite sizes (present work) can replace the infinite domain field. Among these problems are the following:

1. Elastic and elastic-plastic fracture mechanics problems, where cracks of any size, shape and under generalized loading are modeled using distributions of dislocations, in finite size structural elements. Reference [27] contains a list of the most important applications of dislocation theory in fracture. The reader is also advised to check the book written by Lardner [19] as well as Bilby and Eshelby's article [29].
2. Dislocation-crack interaction problems, such as the spread of plastic yield from crack tips [46], cleavage, dislocation emission and crack shielding under generalized loading conditions [47].
3. Problems of micromechanics of plasticity and viscoplasticity (dislocation creep), which involve detailed descriptions of dislocation motion as well as dislocation-dislocation interactions in real crystals or in specimens of finite sizes [15, 16, 48].

A major outcome of the present work is that it demonstrates the weakness of the infinite domain dislocation solution in a large number of problems in which the range of interest for the dislocational field is comparable to the domain size. This is illustrated in Fig. 11, where the stress component σ_{v^*} changes between tensile and compressive on one side of the v^*-axis, which is not a feature of the infinite domain solution. Also, a rotation of the Burger's vector can dramatically change the features of the stress field for the same geometry. This is shown by comparing Figs. 11 and 12. Another important effect is the behavior of the stress field close to the domain corners and edges (Figs. 13 to 15).

It must be noted that the general method developed in this paper is also applicable for

obtaining the Green's function for screw dislocations, and for dislocations of mixed-mode character in finite domains.

A. Dislocational and self-equilibrium conditions

A.1. Dislocational condition

By definition, the Burger's vector is given by the cyclic function of the displacement vector [38] and is written as

$$b_z = [\mathscr{U}_z]_L = \oint_L \mathrm{d}\mathscr{U}_z(z_1, z_2, \bar{z}_1, \bar{z}_2), \tag{40}$$

where $\mathrm{d}\mathscr{U}_z$ is the exact differential of the complex displacement $\mathscr{U}_z$, and L is any contour in the z-plane which encircles the dislocation. Recalling (2) for the displacement in terms of the complex potentials ϕ_{1s} and ϕ_{2s} is the infinite domain, (40) can be rewritten as

$$b_z = p(\lambda_1)[\phi_{1s}(z_1)]_L + p(\bar{\lambda}_1)[\bar{\phi}_{1s}(\bar{z}_1)]_L + p(\lambda_2)[\phi_{2s}(z_2)]_L + p(\bar{\lambda}_2)[\bar{\phi}_{2s}(\bar{z}_2)]_L, \tag{41}$$

where

$$\begin{aligned} [\phi_{js}(z_j)]_L &= \oint_L \left(\frac{\mathrm{d}\phi_{js}(z_j)}{\mathrm{d}z_j}\right) dz_j, \\ [\bar{\phi}_{js}(\bar{z}_j)]_L &= \oint_L \left(\frac{\mathrm{d}\bar{\phi}_{js}(\bar{z}_j)}{\mathrm{d}\bar{z}_j}\right) d\bar{z}_j, \end{aligned} \tag{42}$$

in which $j = 1, 2$. Recalling (6) for the singular potential functions, $\phi_{js}(z_j)$ and $\bar{\phi}_{js}(\bar{z}_j)$, the derivatives in (42) can be written as follows

$$\begin{aligned} \phi'_{js}(z_j) &= \frac{A_j}{z_j - z_{j0}}, \\ \bar{\phi}'_{js}(\bar{z}_j) &= \frac{\bar{A}_j}{\bar{z}_j - \bar{z}_{j0}}. \end{aligned} \tag{43}$$

Substituting back in (42) and carrying out the contour integral, the following expressions for the cyclic functions of $\phi_{js}(z_j)$ and $\bar{\phi}_{js}(\bar{z}_j)$ can be obtained

$$\begin{aligned} [\phi_{js}(z_j)]_L &= 2\pi i A_j, \\ [\bar{\phi}_{js}(\bar{z}_j)]_L &= -2\pi i \bar{A}_j, \end{aligned} \tag{44}$$

which yield the following expression for the Burger's vector

$$b_z = 2\pi i[A_1 p(\lambda_1) - \bar{A}_{1p}(\bar{\lambda}_1) + A_2 p(\lambda_2) - \bar{A}_2 p(\bar{\lambda}_2)], \tag{45}$$

which is (7) of Section 2.

A.2. Self-equilibrium condition

It is shown from the basic principles of elasticity theory that the stress resultant $X + iY$ around a contour is written as [39]

$$X + iY = \oint_L (\sigma_x + i\sigma_{xy})\,\mathrm{d}y - (i\sigma_y + \sigma_{xy})\,\mathrm{d}x, \tag{46}$$

where $X + iY = 0$ in case of a dislocation. Since the stress tensor components are written in terms of the complex variables z_j, rather than x and y, it is more convenient to carry out the integral of (46) in the z_j-planes. For that purpose, Eqns. (4) are recalled for the relation between z_j and x and y. The differential form of those relations yields $\mathrm{d}y = (\mathrm{d}y/\mathrm{d}z_j)\,\mathrm{d}z_j = \mathrm{d}z_j/\lambda_j$ and $\mathrm{d}y = (\mathrm{d}y/\mathrm{d}\bar{z}_j)\,\mathrm{d}\bar{z}_j = \mathrm{d}\bar{z}_j/\bar{\lambda}_j$. Similarly, $\mathrm{d}x = \mathrm{d}z_j = \mathrm{d}\bar{z}_j$. If Eqns. (2) are then used for stress components, the four integrals in (46) can be evaluated as follows

$$\begin{aligned}
&\oint_L \sigma_x\,\mathrm{d}y = 2\pi i(\lambda_1 A_1 - \bar{\lambda}_1 \bar{A}_1 + \lambda_2 A_2 - \bar{\lambda}_2 \bar{A}_2),\\
&i\oint_L \sigma_{xy}\,\mathrm{d}y = 2\pi(A_1 - \bar{A}_1 + A_2 - \bar{A}_2),\\
&-\oint_L \sigma_{xy}\,\mathrm{d}y = 2\pi i(\lambda_1 A_1 - \bar{\lambda}_1 \bar{A}_1 + \lambda_2 A_2 - \bar{\lambda}_2 \bar{A}_2),\\
&-\mathrm{i}\oint_L \sigma_y\,\mathrm{d}y = 2\pi x(A_1 - \bar{A}_1 + A_2 - \bar{A}_2).
\end{aligned} \tag{47}$$

Substituting the above expressions in (46) and recalling that $\gamma_j = 1 - i\lambda_i$ and $\delta_j = 1 + i\lambda_j$, the following equation is obtained

$$\delta_1 A_1 - \bar{\gamma}_1 \bar{A}_1 + \delta_2 A_2 - \bar{\gamma}_2 \bar{A}_2 = 0, \tag{48}$$

where a factor of 4π is cancelled. The last equation is just (8) of Section 2.

B. Solution for $\lambda_{1,2}$ and $A_{1,2}$ in orthotropic media

B.1. Solution for $\lambda_{1,2}$

For orthotropic media $s_{16} = s_{26} = 0$ and the characteristic equation (3) of Section 2 reduces to

$$s_{11}\lambda^4 + (2s_{12} + s_{66})\lambda^2 + s_{22} = 0, \tag{49}$$

which has imaginary roots. The roots of (49) occur in conjugate pairs and are given by λ_1 and $\bar{\lambda}_1 = \pm i\beta_1$ and λ_2 and $\bar{\lambda}_2 = \pm i\beta_2$ where β_1 and β_2 are given by

$$\begin{aligned} \beta_1^2 &= |-r_1 + \sqrt{r_1^2 - r_2}|, \\ \beta_2^2 &= |-r_1 + \sqrt{r_1^2 - r_2}|, \end{aligned} \tag{50}$$

where r_1 and r_2 are given by

$$r_1 = \left(\frac{2s_{12} + s_{66}}{2s_{11}}\right), \quad r_2 = \left(\frac{s_{22}}{s_{11}}\right). \tag{51}$$

B.2. Solution for $A_{1,2}$

The dislocation and self-equilibrium conditions yield the two equations (45) and (48) for the two complex constants A_1 and A_2. By taking the complex conjugates of the two equations, two additional equations are obtained. The four equations can then be solved for A_1, A_2, $\bar{A}_1$ and $\bar{A}_2$. Due to the self-equilibrium condition the following two equations can be written

$$\begin{aligned} &\delta_1 A_1 - \bar{\gamma}_1 \bar{A}_1 + \delta_2 A_2 - \bar{\gamma}_2 \bar{A}_2 = 0, \\ &\bar{\delta}_1 \bar{A}_1 - \gamma_1 A_1 + \bar{\delta}_2 \bar{A}_2 - \gamma_2 A_2 = 0. \end{aligned} \tag{52}$$

As mentioned before, $\lambda_j = i\beta_j$ are imaginary quantities. Consequently, the parameters $\gamma_j = 1 - i\lambda_j = 1 + \beta_j = \bar{\gamma}_j$ and $\delta_j = 1 + i\lambda_j = 1 - \beta_j = \bar{\delta}_j$ are real quantities. Substituting these back in (52), and separating the real and imaginary parts, the following two equations are obtained for the real and imaginary parts of A_1 and A_2

$$\begin{aligned} &\beta_1 \operatorname{Re}(A_1) + \beta_2 \operatorname{Re}(A_2) = 0, \\ &\operatorname{Im}(A_1) + \operatorname{Im}(A_2) = 0. \end{aligned} \tag{53}$$

The dislocational condition yields the following two equations

$$\begin{aligned} &p(\lambda_1)A_1 - p(\bar{\lambda}_1)\bar{A}_1 + p(\lambda_2)A_2 - p(\bar{\lambda}_2)\bar{A}_2 = \frac{b}{2\pi i}, \\ &\bar{p}(\bar{\lambda}_1)\bar{A}_1 - \bar{p}(\lambda_1)A_1 + \bar{p}(\bar{\lambda}_2)\bar{A}_2 - \bar{p}(\lambda_2)A_2 = \frac{\bar{b}}{-2\pi i}. \end{aligned} \tag{54}$$

It can be shown that $p(\lambda_j)$, $p(\bar{\lambda}_j)$ and their respective conjugates, $\bar{p}(\bar{\lambda}_j)$ and $\bar{p}(\lambda_1)$, are real constants in the case of orthotropic media, where λ_j are imaginary. However, these quantities are found in terms of β_1 and β_2. Using (54) and excluding algebraic details, the following two

equations are obtained for the real and imaginary parts of A_1 and A_2

$$\begin{aligned}
&\alpha_1 \operatorname{Re}(A_1) + \alpha_2 \operatorname{Re}(A_2) = \frac{\operatorname{Im}(b)}{2\pi}, \\
&\alpha_3 \operatorname{Im}(A_1) + \alpha_4 \operatorname{Im}(A_2) = -\frac{\operatorname{Re}(b)}{2\pi},
\end{aligned} \tag{55}$$

where $\alpha_{1,2,3,4}$ are written in terms of $\beta_{1,2}$ and s_{ij} as follows

$$\begin{aligned}
\alpha_1 &= \frac{2}{\beta_1}(s_{22} - s_{12}\beta_1^2), \\
\alpha_2 &= \frac{2}{\beta_2}(s_{22} - s_{12}\beta_2^2), \\
\alpha_3 &= 2(s_{12} - s_{11}\beta_1^2), \\
\alpha_4 &= 2(s_{12} - s_{12}\beta_2^2).
\end{aligned} \tag{56}$$

Equations (53) and (55) are four algebraic equations in four unknowns, $\operatorname{Re}(A_1)$, $\operatorname{Re}(A_2)$, $\operatorname{Im}(A_1)$, and $\operatorname{Im}(A_2)$, which are easy to solve. Expressions for A_1 and A_2 are written as follows

$$\begin{aligned}
A_1 &= \frac{-\beta_2 \operatorname{Im}(b)}{2\pi(\beta_1\alpha_2 - \beta_2\alpha_1)} + i\frac{-\operatorname{Re}(b)}{2\pi(\alpha_3 - \alpha_4)}, \\
A_2 &= \frac{\beta_1 \operatorname{Im}(b)}{2\pi(\beta_1\alpha_2 - \beta_2\alpha_1)} + i\frac{\operatorname{Re}(b)}{2\pi(\alpha_3 - \alpha_4)},
\end{aligned} \tag{57}$$

which can be rewritten as

$$\begin{aligned}
A_1 &= c_{11} \operatorname{Im}(b) + ic_{12} \operatorname{Re}(b) \\
A_2 &= c_{21} \operatorname{Im}(b) + ic_{22} \operatorname{Re}(b)
\end{aligned} \tag{58}$$

C. The elliptic function of Jacobi, *sn*(*w*, *k*)

Equation (37), which gives z in terms of w, is known as the elliptic sine function of Jacobi. For the reader's convenience, the properties of that function, which were used for computational purposes in the present work, are extracted from [44] and [45] and summarized in this appendix. Two other elliptic functions, $cn(w, k)$ and $dn(w, k)$, are related to $sn(w, k)$ as follows

$$\begin{aligned}
&cn^2(w, k) + sn^2(w, k) = 1, \\
&dn^2(w, k) + k^2 sn^2(w, k) = 1,
\end{aligned} \tag{59}$$

where k is a parameter. In the case of the purely imaginary argument, $w = vi$, the following properties were used

$$sn(vi, k) = i\frac{sn(v, k')}{cn(v, k')},$$

$$cn(vi, k) = \frac{1}{cn(v, k')}, \tag{60}$$

$$dn(vi, k) = \frac{dn(v, k')}{cn(v, k')},$$

where $k^2 + k'^2 = 1$. The addition property of the function $sn(u \pm v)$ is written as

$$sn(u \pm v) = \frac{sn(u)cn(v)dn(v) \pm cn(u)sn(v)dn(u)}{1 - k^2 sn^2(u)sn^2(v)}, \tag{61}$$

where k is dropped from both sides for simplicity. In the case of a complex argument $w = u + iv$, which is considered in the present work, v is replaced by iv in (61) and Eqns. (60) are used, which yields the following expression for $sn(w, k)$ in terms of the elliptic functions of the real and imaginary parts of w

$$sn(w, k) = \frac{sn(u, k)dn(v, k') + icn(u, k)cn(v, k')sn(v, k')dn(u, k)}{cn^2(v, k') + k^2 sn^2(u, k)sn^2(v, k')}, \tag{62}$$

in which the functions dn and cn are evaluated in terms of sn using (59). The function sn can be evaluated in terms of circular or hyperbolic functions using the descending (decrease k) or ascending (increase k) Landen transformation, respectively [44]. The accuracy of the calculations depends on the order of transformation used. However, both methods were tried for the present work and yielded significant computational errors. A series expansion for the function $sn(u, k)$ in terms of the nome $q = e^{-\pi K'/K}$ and the argument $u' = \pi u/(2K)$ is used in the present work, which is written as

$$sn(u, k) = \frac{2\pi}{kK} \sum_{n=0}^{\infty} \frac{q^{n+1/2}}{1 - q^{2n+1}} \sin(2n + 1)u' \tag{63}$$

where K is the complete elliptic integral of the first kind defined by (29) and $K' = K(k')$. The series converges depending on the value of q which, in turn, depends on the ratio K'/K, i.e. on the geometry of the rectangle. However, a range of $n = 10 - 15$ was adequate for the computational purposes in the present work.

References

1. G. Weingarten, *Atti Accademia Nazionale die Lincie* 10 (1901) 57–61.
2. A. Timpe, *Zeitschrift fur Mathematik und Physik* 52 (1905) 348–383.
3. V. Volterra, *Annale Scientifiques de l'Ecole Normale Superieure* (Paris) 24 (1907) 401–517.

4. A.E.H. Love, *A Treatise on the Mathematical Theory of Elasticity*, Cambridge University Press, Cambridge (1927).
5. Th. v. Karman and L. Föppl, *Enzyklopadie Der Mathematischen Wissenchaften Mechanik* 4 (1913) 695–770.
6. L. Prandtl, *Zeitschrift fur Angewandte Mathematik und Mechanik* 8 (1923) 85–106.
7. G.I. Taylor, *Transactions of the Faraday Society* 24 (1928) 121–125.
8. E. Orowan, *Diplomarbeit*, T.H.S. Berlin (1929).
9. J.P. Hirth and J. Lothe, *Theory of Dislocations*, Second Edition, John Wiley and Sons (1982).
10. F.R.N. Nabarro, *Dislocations in Solids*, North-Holland Publishing Company (1979).
11. M.J. Marcinkowski et al, *Physica Status Solidi* (a) 17 (1973) 423–433.
12. M.J. Marcinkowski et al, *Physica Status Solidi* (a) 18 (1973) 361–375.
13. K. Jagannadham and M.J. Marcinkowski, *Journal of Materials Science* 15 (1980) 563–574.
14. K. Jagannadham and M.J. Marcinkowski, *Journal of Materials Science* 14 (1979) 1717–1732.
15. R.J. Amodeo and N.M. Ghoniem, *Physical Review B*, 41 (1990) 6958–6967.
16. R.J. Amodeo and N.M. Ghoniem, *Physical Review B*, 41 (1990) 6968–6976.
17. T. Mura, in *Advances in Materials Research*, vol. 3, H. Herman (ed.), John Wiley and Sons (1968) 1–108.
18. T. Mura, *Micromechanics of Defects in Solids*, Martinus Nijhoff Publishers (1987).
19. R.W. Lardner, *Mathematical Theory of Dislocations and Fractu e*, University of Toronto Press (1974).
20. A.N. Stroh, *Philosophical Magazine* 3 (1958) 625–646.
21. J. Qu and Q. Li, *Journal of Elasticity* 26 (1991) 169–195.
22. J.R. Willis, *Journal of the Mechanics and Physics of Solids* 19 (1971) 353–368.
23. F. Delale and F. Erdogan, *International Journal of Fracture* 20 (1982) 251–265.
24. R.W. Lardner, *International Journal of Fracture Mechanics* 4 (1968) 299–319.
25. C. Atkinson, *International Journal of Fracture Mechanics* 2 (1968) 567–575.
26. V. Vitek, *International Journal of Fracture* 13 (1977) 481–501.
27. V. Vitek and G.G. Chell, in *Dislocation Modelling in Physical Systems*, Proceedings of International Conference, Gainesville, Florida, USA, June 22–27, 1986, M.F. Ashby, R. Boullough, C.S. Hartly, and J.P. Hirth (eds.) 92–109.
28. K. Jagannadham and M.J. Marcinkowski, *Unified Theory of Fracture*, Trans Tech Publications (1983).
29. B.A. Bilby and J.D. Eshelby, in *Fracture, An Advanced Treatise*, Vol. 1, H. Liebowitz (ed.), Academic Press, New York and London (1968) 99–182.
30. K. Jagannadham and M.J. Marcinkowski, *Physica Status Solidi* (a) 50 (1978) 293–302.
31. K. Jagannadham and M.J. Marcinkowski, *Journal of Materials Science* 14 (1979) 1052–1070.
32. K. Jagannadham and M.J. Marcinkowski, *Materials Science and Engineering* 38 (1979) 259–270.
33. G.R. Miller, *Journal of Applied Mechanics* 53 (1986) 368–389.
34. J.C. Lee, *Engineering Fracture Mechanics* 37 (1990) 209–219.
35. L. Volkovyski, G. Lunts and I. Aramanovich, *Problems in the Theory of Functions of a Complex Variable*, Mir Publishers, Moscow (1972).
36. Zeev Nehari, *Conformal Mapping*, Dover Publications Inc, New York (1952).
37. Ruel V. Churchill and James Ward Brown, *Complex Variables and Applications*, Fifth Edition, McGraw-Hill (1990).
38. L.M. Milne-Thomson, *Plane Elastic Systems*, Springer Verlag (1968).
39. N.I. Muskhelishvili, *Some Basic Problems of the Mathematical Theory of Elasticity*, P. Noordhoff Ltd. (1963).
40. N.I. Muskhelishvili, *Singular Integral Equations*, Moscow (1946).
41. R. Solecki, in *Yamada Conference IX on Dislocations in Solids*, H. Suzuki (ed.), University of Tokyo Press (1985) 25–28.
42. J.A. Dicarlo and Gregory N. Morscher, in *Failure Mechanisms in High Temperature Composite Materials*, AD-Vol-122, ASME (1991) 15–22.
43. T.D. Gulden, *Journal of the American Ceramic Society* 52 (1969) 585–590.
44. M. Abramowitz and I.A. Stegun, *Handbook of Mathematical Functions with Formulas, Graphs and Mathematical Tables*, Ninth Edition, Dover Publication, Inc, New York (1972).
45. Harold T. Davis, *Introduction to Nonlinear Differential and Integral Equations*, Dover Publications Inc, New York (1962).
46. V. Vitek, *Journal of the Mechanics and Physics of Solids* 24 (1975) 67–76.
47. I.-H. Lin and R. Thomson, *Acta Metallurgica* 34 (1986) 187–206.
48. E.H. Jordan and K.P. Walker, *Journal of Engineering Materials and Technology* ASME 114 (1992) 19–26.